Journal of Materials Chemistry B

Mesoscopic Heterogeneity in Nanocellulose-Containing Cell Storage Medium

Journal:	*Journal of Materials Chemistry B*
Manuscript ID	TB-COM-01-2020-000219.R2
Article Type:	Communication
Date Submitted by the Author:	24-Mar-2020
Complete List of Authors:	Shundo, Atsuomi; Kyushu University, Applied Chemistry Matsumoto, Yuji; Kyushu University, Applied Chemistry Hayashi, Hisato; Nissan Chemical Corporation Tsuruzoe, Nobutomo; Nissan Chemical Corporation Matsuno, Hisao; Kyusyu University, Department of Applied Chemistry Tanaka, Keiji; Kyushu University, Department of Applied Chemistry

COMMUNICATION

Mesoscopic Heterogeneity in Nanocellulose-Containing Cell Storage Medium

Received 00th January 20xx,
Accepted 00th January 20xx

DOI: 10.1039/x0xx00000x

Atsuomi Shundo,*[a,b,c] Yuji Matsumoto,[b] Hisato Hayashi,[d] Nobutomo Tsuruzoe,[d] Hisao Matsuno,[b,c,e] and Keiji Tanaka*[a,b,c,e]

Nanocellulose (NC)-containing medium is one of the promising candidates for cell storage that allows cell floating without any stirring. We here found that the NC medium was spatially heterogeneous in terms of its rheological properties. The characteristic length of the heterogeneity was a few tens of micrometers and it decreased upon sonication treatment. The length scale of the heterogeneity affected the cell suspension; the NC medium having smaller length scale suppressed the cell sedimentation effectively.

Nanocellulose (NC) is a class of shape-anisotropic materials with a diameter of several tens of nanometers and a length of over several hundreds of nanometers.[1] Since NC is generally extracted from natural resources such as wood pulp and cotton, it exhibits good biocompatibility including low cytotoxicity to human cell lines.[2] Thus, NC has been used as a building block for biomedical applications such as scaffolds for cell culturing,[3] templates for biomineralization of hydroxyapatite[4] and membranes for wound dressing.[5]

So far, great efforts have been devoted to cell culture using NC-based scaffolds such as electrospun fibers,[6] and aerogels.[7] In these cases, NC provides the interactive surface which promotes cell adhesion and growth. On the other hand, a non-adherent cell culture utilizing NC-based scaffolds has been also made. One such example is the three-dimensional culture of stem cells in a hydrogel composed of NC.[8] During cell proliferation, cells are uniformly distributed in suspension over the entire region of the hydrogel thanks to the network structure of NC.

Recently, it has been reported that mesenchymal stem cells can be floated in a NC-containing culture medium, which is macroscopically not a gel but a fluid due to the low concentration of NC.[9] The NC-containing medium can be characterized by the fact that stirring it is not necessarily required for cell floating and floated stem cells maintain their functions without showing any loss of viability and deterioration of differentiation. These features make the NC-containing medium a promising candidate for a cell storage medium, which would be useful for the practical stage of regenerative medicine. Notably, the cell storage in the NC-containing medium differs from a conventional freezing approach, which often causes physical damage to stem cells.[10] To accelerate the application of the NC-containing medium for cell storage, its structure and physical properties should be studied as the first benchmark.

We have previously examined local rheological properties of the aqueous dispersion of NC by a particle tracking experiment[11] in which the thermal motion of a probe particle embedded in a material of interest was tracked.[12] The observation for individual particles at different locations revealed that the NC aqueous dispersion was spatially heterogeneous in terms of its rheological properties. Varying the particle size, the characteristic length scale of the heterogeneity was found to be in the order of several tens of micrometers. To gain a better understanding of the cell suspension properties, in this study, we examine whether the heterogeneity exists even for the NC-containing medium and how the heterogeneity affects suspension properties if at all.

An aqueous dispersion of NC was prepared from a crystalline cellulose powder obtained by an aqueous counter collision method.[9,13] The average width and length of NC were 21 ± 3 and 460 ± 200 nm, respectively.[11] Water in the NC dispersion was replaced by a normal Roswell Park Memorial Institute (RPMI) 1640 medium via repeating cycles of centrifugation and decantation (see ESI†). The addition of NC did not change pH of the medium, as confirmed by the colour of phenolphthalein in it. The NC-containing medium with a concentration of 0.1 wt% was sonicated for 1 hour and then left undisturbed (aging) at 298 K for 72 hours. The appearance of the NC-containing medium stayed transparent during sonication treatment, suggesting that there was no scattering of visible light. The viscosity of the

[a] *Department of Automotive Science,* [b] *Department of Applied Chemistry,* [c] *International Institute for Carbon-Neutral Energy Research (WPI-I2CNER), and* [e] *Center for Polymer Interface and Molecular Adhesion Science, Kyushu University, Fukuoka 819-0395, Japan.*
[b] *E-mail: a-shundo@cstf.kyushu-u.ac.jp (A.S.); k-tanaka@cstf.kyushu-u.ac.jp (K.T.)*
[d] *Nissan Chemical Corporation, Tokyo 101-0054, Japan.*
† Electronic Supplementary Information (ESI) available: Details of experimental procedures, confocal microscopic observation. See DOI: 10.1039/x0xx00000x

original NC medium was 1.1 mPa·s, and was comparable to that of the medium without NC. After sonication and successive aging, however, the viscosity increased to 5.6 mPa·s. Such an increase in the viscosity was also observed for the aqueous dispersion of NC, which did not contain any constituents of RPMI 1640 such as salts and amino acids.[11] Thus, it is apparent that the viscosity increase observed here was induced not by the presence of the culture medium but NC itself.

To examine the rheological properties of the NC media at various length scales, we here employed particle tracking measurement using polystyrene (PS) particles with various diameters (d) ranging from 1 μm to 45 μm, as a probe. The thermal motion of PS particles embedded in the NC medium was tracked using our setup based on inverted microscopy, as reported elsewhere (see ESI†).[11,12c,14] Based on two-dimensional trajectories of PS particles, the mean-square displacement, $\langle \Delta r^2(t) \rangle$ was obtained from the following equation;[12b]

$$\left\langle \Delta r^2(t) \right\rangle = \frac{1}{N}\sum_{i=1}^{N}\left\{ \boldsymbol{r}_i(t) - \boldsymbol{r}_i(0) \right\}^2 \quad (1)$$

where $r_i(t)$ is the position of a particle i at time t, $r_i(0)$ is the initial position and N is the number of data analyzed. Using the slope (n) of the double logarithmic plot of $\langle \Delta r^2(t) \rangle$ against t, the type of particle motion can be discussed.[12b,15] A slope equal to 1 means that the motion of particles is based on the random walk statistical model, as is commonly seen for particle diffusion in a homogeneous Newtonian liquid.[12b,15b] By contrast, a slope less than 1 indicates that particles moved in a sub-diffusive manner, which was generally explained in terms of the trapping of particles within the structure formed in the material.[15b]

Fig. 1a shows the double logarithmic plots of $\langle \Delta r^2(t) \rangle$ against t for PS particles in the original NC medium. Each solid line was obtained by monitoring a single particle 10 times and then taking an average of them. The slope of the hypotenuse of the right-angled triangle in the figure corresponds to 1. For a particle with d = 1 μm, the n value for all plots was 1, meaning that the diffusion of particles followed the random walk statistical model. With increasing particle size, the possibility of n being less than 1 increased. For a particle with d = 45 μm, consequently, the n for all plots became zero. This was probably because the aggregation structure of NC suppressed the particle motion.[11,15b]

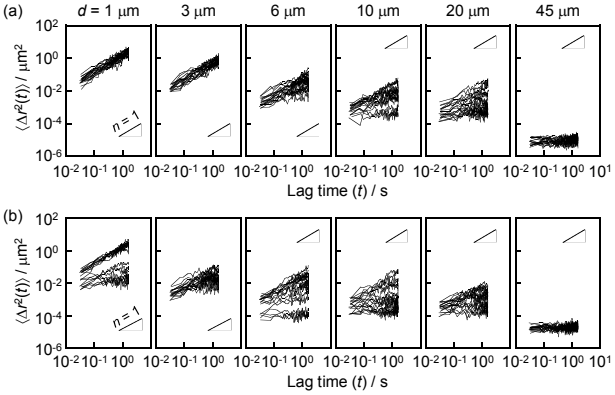

Fig. 1 Double logarithmic plots of $\langle \Delta r^2(t) \rangle$ against t for PS particles with diameters of 1, 3, 6, 10, 20 and 45 μm embedded in (a) the original NC medium and (b) the medium after sonication treatment. The slope of the hypotenuse of triangles corresponds to unity.

Here, it is noteworthy that there was a variation in the n value for particles having d = 6, 10 and 20 μm. This suggests that in these cases, some particles diffused normally and others were restricted because they were not located in an equivalent environment.

Fig. 1b shows the plots of $\langle \Delta r^2(t) \rangle$ against t for PS particles in the NC medium obtained after sonication treatment. Similarly to the original NC dispersion, the n value decreased with increasing particle size. The n variation for the $\langle \Delta r^2(t) \rangle$ plot was also observed. However, the particle diameter showing the variation seems to differ from that of the original NC medium. To clarify such a difference, a non-Gaussian parameter, $\alpha_2(t)$, was here adopted as follows;[14c,16]

$$\alpha_2(t) = \frac{3}{5}\frac{\left\langle \Delta r^4(t) \right\rangle}{\left\langle \Delta r^2(t) \right\rangle^2} - 1 \quad (2)$$

where $\langle \Delta r^4(t) \rangle$ is the fourth moment of a particle displacement. The $\alpha_2(t)$ value is a measure of the deviation from a Gaussian distribution of the particle displacement. A greater $\alpha_2(t)$ corresponds to a system that is more heterogeneous.[14c,16a]

Fig. 2 shows the correlation between d and $\langle \alpha_2(t) \rangle$ for the original NC medium and the one after sonication treatment. The $\langle \alpha_2(t) \rangle$ value corresponds to $\alpha_2(t)$ averaged over lag times ranging from 0 to 1.6 s, provided that no substantial increase in $\alpha_2(t)$ with t was observed. For the original NC medium, the $\langle \alpha_2(t) \rangle$ value at d = 1 μm was near to zero, meaning that the system looked to be homogeneous at this length scale. With increasing particle size, the $\langle \alpha_2(t) \rangle$ value increased and then decreased. The maximum value was observed at d = 20 μm. It is obvious that the NC medium was heterogeneous at the length scale of a few tens of micrometers. For the NC medium obtained after sonication treatment, a finite value of $\langle \alpha_2(t) \rangle$ was also observed. However, the d value, at which $\langle \alpha_2(t) \rangle$ was maximized, was 10 μm. Hence, it is most likely that the length scale of the heterogeneity decreased because of sonication treatment. Taking into account that the size of cells was in the range of 10–20 μm,[17] sonication treatment should affect the cell suspension properties of the NC medium. This hypothesis motivated us to examine the cell suspension properties in the NC media with and without sonication treatment, having shorter and longer length scale of the heterogeneity, respectively, as discussed in the next paragraph.

As a probe for the cell suspension properties, mouse fibroblast L929 cells, which were classified as adherent cells, were used because they were generally capable of responding to

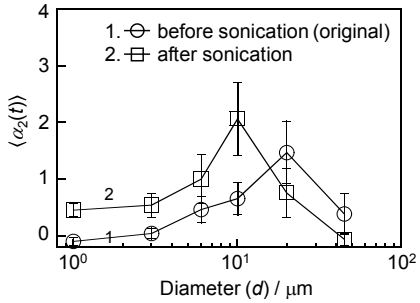

Fig. 2 Correlation between d and $\langle \alpha_2(t) \rangle$ for PS particles embedded in the original NC medium and the medium after sonication treatment.

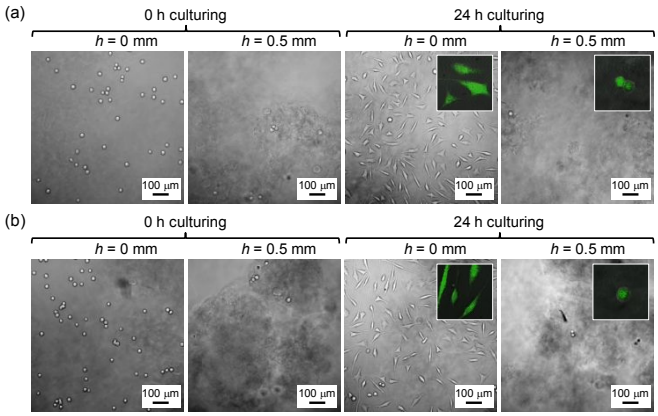

Fig. 3 Representative CLSM images acquired at h of 0 and 0.5 mm for (a) the original NC medium and (b) the medium after sonication treatment. The observations were made after culturing for 0 and 24 hours. Insets denote fluorescence microscopic images for L929 cells stained with Calcein-AM and EthD-1 after culturing for 24 hours.

the chemical and/or physical stimuli.[18] Cells were seeded to the NC medium at 1.0 x 10^5 cells·mL^{-1} (see ESI†). Z-stack images were acquired from the liquid surface to the bottom of a media with an interval of 10 μm between each image (see ESI†). **Fig. 3a** shows representative confocal laser scanning microscopic (CLSM) images acquired at h of 0 and 0.5 mm, where h denotes the height distance of the focal plane from the bottom of the well, for the original NC medium. At a culturing time of 0 hours, cells were spherical in their shape both at h of 0 and 0.5 mm. After 24 hours, they had spread out at h of 0 mm, implying their rigid adhesion to the bottom of the well. On the other hand, they maintained their spherical shape at h of 0.5 mm. These findings were also seen for the NC medium after sonication treatment, as shown in **Fig. 3b**. The spherical shape of cells located at h of 0.5 μm suggests that NC aggregates do not act as an adhesive scaffold for L929 cells. Here, to address the cell viability in the NC medium, fluorescence images were acquired for cells stained with a LIVE/DEAD solution after curing for 24 hours (see ESI†).[19] Living cells were observed at h of 0 and 0.5 mm, as evidenced by the green color in the insets of **Fig. 3**. The mortality rate was less than 1 %, meaning that NC was not toxic for L929 cells.

To quantify the cell suspension properties, cell floating ratio (ϕ), which can be defined as a ratio of the number of cells at $h >$ 0 to the total number of cells, was estimated. **Fig. 4** shows culturing time vs. ϕ for the original NC medium and one after sonication treatment. In this culturing time range, since the cell proliferation did not occur, the total number of cells was almost unchanged. For the RPMI 1460 medium without NC, the ϕ value was zero regardless of time, meaning that all cells settled to the bottom. Conversely, for the original NC medium, the ϕ value at 0 h culturing was ca. 50 % and it exponentially decreased with increasing time. Such a decrease in ϕ was also observed for the NC medium after sonication treatment. However, the ϕ decrease was substantially slower than that for the original one. Also, cells at $h > 0$ were observed even after 72 h culturing. These results indicate that the addition of NC into the medium

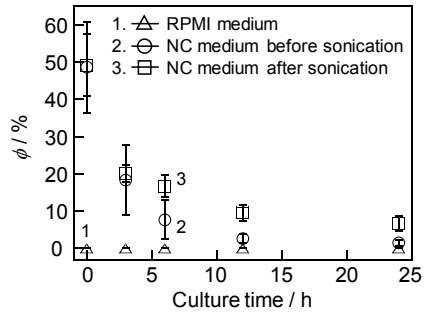

Fig. 4 Time-dependence of ϕ for the pure RPMI1640 medium, the original NC medium and the medium after sonication treatment.

suppressed the cell sedimentation and the suppression was more effective after sonication.

To discuss why there was a difference in ϕ and a longer and shorter length scale of heterogeneity before and after sonication, respectively, the heterogeneous aggregation structure was directly imaged by CLSM observation with Rhodamine 6G (R6G) as a fluorescence probe (see ESI†).[11] The adsorption of R6G on the NC surface gives a contrast in the CLSM image.[20] For the original NC medium, denser and less-dense regions of NC were expressly distinguishable. After sonication, the areal size of the denser regions increased and that of the less-dense ones concurrently decreased although a quantitative measurement of their size was difficult.[21] In our previous study, it was found that the size and chemical state of NC remained unchanged even after the sonication treatment.[11] Also, wide-angle X-ray diffraction (WAXD) measurements confirmed that the degree of the crystallinity of NC kept its original value after the sonication (see ESI†). Thus, an increase in the size of the denser regions should be a result of not the change of individual NC but the dissociation of NC aggregates.

The heterogeneity detected by particle tracking can be associated with the location-dependent density of NC. Particles located in the denser regions are dynamically constrained while others in the less-dense regions are not.[16b,22] Once the denser regions apparently evolve upon sonication, or the less-dense regions devolve, particles can be difficult to incorporate into the less-dense regions with their reduced size. This means that particles are supposed to be more partitioned into the denser regions, in which the real NC density decreases due to a better dispersion state.

The above picture can explain the relationship between heterogeneity and cell suspension properties. After cell seeding, cells are uniformly distributed to the denser and less-dense regions of NC. Whereas cells in denser regions are expected to be in a floating state, ones in less-dense regions sink. As mentioned above, cells do not strongly adhere to NC and its aggregates. Thus, cells in the denser region can diffuse out of the regions and start to sink. After a while, cells would be re-trapped by another denser region. Given that the cycle of sink and re-trap is repeated, the ϕ decrease with increasing time seen in **Fig. 4** can be reasonably understood. Accordingly, the slow ϕ decrease observed after sonication treatment can be attributed to the expansion of the dense regions.

In conclusion, we applied a particle tracking experiment to a NC-containing medium, which was one of the promising candidates for cell storage media. The observation for individual particles at different locations revealed that the NC medium was spatially heterogeneous in terms of its rheological properties and the characteristic length was a few tens of micrometers. Notably, the length scale of the heterogeneity decreased upon sonication and the successive aging at room temperature. The suspension properties of the NC media with and without sonication treatment, having shorter and longer length scale of the heterogeneity, respectively, were also examined using L929 cells as a probe. The addition of NC into the medium suppressed the cell sedimentation and the suppression was more effective after sonication. This finding can be attributed to the size change of the heterogeneous structure, or the denser and less-dense regions of NC. The knowledge obtained here should be useful for understanding and controlling the cell suspension, thereby leading to the design of cell storage media.

Acknowledgements

This research was partly supported by JSPS KAKENHI, Grant-in-Aid for Scientific Research (B) (no. JP19H02780) (A.S.) and JST-Mirai Program (JPMJMI18A2) (K.T.). The synchrotron radiation facilities experiments were performed at BL40B2 in the SPring-8 with the approval of the Japan Synchrotron Radiation Research Institute (JASRI) (Proposal: 2015A1748 and 2015B1665).

Conflicts of interest

There are no conflicts to declare.

Notes and references

1 (a) R. J. Moon, A. Martini, J. Nairn, J. Simonsen and J. Youngblood, *Chem. Soc. Rev.*, 2011, **40**, 3941−3994: (b) D. Klemm, F. Kramer, S. Moritz, T. Lindström, M. Ankerfors, D. Gray and A. Dorris, *Angew. Chem., Int. Ed*., 2011, **50**, 5438−5466.

2 (a) G. Helenius, H. Bäckdahl, A. Bodin, U. Nannmark, P. Gatenholm and B. Risberg, *J. Biomed. Mater. Res*., 2006, **76**, 431–438; (b) T. Kovacs, V. Naish, B. O'Connor, C. Blaise, F. Gagné, L. Hall, V. Trudeau and P. Martel, *Nanotoxicology*, 2010, **4**, 255−270; (c) K. B. Male, A. C. W. Leung, J. Montes, A. Kamen and J. H. T. Luong, *Nanoscale*, 2012, **4**, 1373−1379; (d) S. F. Souza, A. L. Leao, C. B. Lombello, M. Sain and M. Ferreira, *J. Mater. Sci.*, 2017, **52**, 2581−2590; (e) S. F. Souza, M. Mariano, D. Reis, C. B. Lombello, M. Ferreira and M. Sain, *Carbohydr. Polym.*, 2018, **201**, 87−95.

3 (a) R. M. A. Domingues, M. E. Gomes and R. L. Reis, *Biomacromolecules*, 2014, **15**, 2327−2346; (b) K. Hua, I. Rocha, P. Zhang, S. Gustafsson, Y. Ning, M. Strømme, A. Mihranyan and N. Ferraz, *Biomacromolecules*, 2016, **17**, 1224−1233; (c) D. Nguyen, D. A. Hägg, A. Forsman, J. Ekholm, P. Nimkingratana, C. Brantsing, T. Kalogeropoulos, S. Zaunz, S. Concaro, M. Brittberg, A. Lindahl, P. Gatenholm, A. Enejder and S. Simonsson, *Sci. Rep*. 2017, **7**, 658; (d) Y. P. Singh, A. Bandyopadhyay and B. B. Mandal, *ACS Appl. Mater. Interfaces,* 2019, **11**, 33684−33696.

4 (a) S. Shi, S. Chen, X. Zhang, W. Shen, X. Li, W. Hu, and H. Wang, *J. Chem. Technol. Biotechnol.,* 2009, **84**, 285–290; (b) S. Morimune-Moriya, S. Kondo, A. Sugawara-Narutaki, T. Nishimura, T. Kato and C. Ohtsuki, *Polym. J*., 2015, **47**, 158–163.

5 (a) W. Czaja, A. Krystynowicz, S. Bielecki and R. Brownjr, *Biomaterials*, 2006, **27**, 145–151; (b) C. Xu, B. Z. Molino, X. Wang, F. Cheng, W. Xu, P. Molino, M. Bacher, D. Su, T. Rosenau, S. Willför and G. Wallace *J. Mater. Chem. B*, 2018, **6**, 7066–7075.

6 X. He, Q. Xiao, C. Lu, Y. Wang, X. Zhang, J. Zhao, W. Zhang, X. Zhang and Y. Deng, *Biomacromolecules*, 2014, **15**, 618−627.

7 (a) H. Cai, S. Sharma, W. Liu, W. Mu, W. Liu, X. Zhang and Y. Deng, *Biomacromolecules*, 2014, **15**, 2540−2547; (b) J. Liu, F. Cheng, H. Grénman, S. Spoljaric, J. Seppälä, J. E. Eriksson, S. Willför and C. Xu, *Carbohydr. Polym*., 2016, **148**, 259–271; (c) C. Zhang, T. Zhai, L.-S. Turng, *Cellulose*, 2017, **24**, 2791–2799.

8 (a) M. Bhattacharya, M. M. Malinen, P. Lauren, Y.-R. Lou, S. W. Kuisma, L. Kanninen, M. Lille, A. Corlu, C. GuGuen-Guillouzo, O. Ikkala, A. Laukkanen, A. Urtti and M. Yliperttula, *J. Control. Release*., 2012, **164**, 291–298; (b) M. M. Malinen, L. K. Kanninen, A. Corlu, H. M. Isoniemi, Y.-R. Lou, M. L. Yliperttula and A. O. Urtti, *Biomaterials*, 2014, **35**, 5110–5121; (c) Y.-R. Lou, L. Kanninen, T. Kuisma, J. Niklander, L. A. Noon, D. Burks, A. Urtti and M. Yliperttula, *Stem Cells Dev*., 2014, **23**, 380–392.

9 S. Kidoaki, Y. Tuji, H. Hayashi, T. Iwama, M. Horikawa, *Pat*., WO2015111734A1, 2015.

10 (a) B. Grout, J. Morris and M. McLellan, *Trends Biotechnol*., 1990, **8**, 293–297; (b) E. R. Garvican, S. Cree, L. Bull, R. K. W. Smith and J. Dudhia, *Stem Cell Res. Ther*., 2014, **5**, 94-1–10.

11 Y. Matsumoto, A. Shundo, H. Hayashi, N. Tsuruzoe and K. Tanaka, *Macromolecules*, 2019, **52**, 8266−8274.

12 (a) M. T. Valentine, P. D. Kaplan, D. Thota, J. C. Crocker, T. Gisler, R. K. Prud'homme, M. Beck and D. A. Weitz, *Phys. Rev. E: Stat. Phys., Plasmas, Fluids, Relat. Interdiscip. Top*., 2001, **64**, 061506-1−9; (b) T. A. Waigh, *Rep. Prog. Phys*., 2005, **68**, 685−742; (c) D. P. Penaloza, K. Hori, A. Shundo and K. Tanaka, *Phys. Chem. Chem. Phys*., 2012, **14**, 5247−5250.

13 R. Kose, I. Mitani, W. Kasai and T. Kondo, *Biomacromolecules*, 2011, **12**, 716−720.

14 (a) A. Shundo, K. Mizuguchi, M. Miyamoto, M. Goto and K. Tanaka, *Chem. Commun*., 2011, **47**, 8844–8846; (b) A. Shundo, K. Hori, D. P. Penaloza, Y. Matsumoto, Y. Okumura, H. Kikuchi, K. E. Lee, S. O. Kim and K. Tanaka, *Phys. Chem. Chem. Phys*., 2016, **18**, 22399−22406; (c) Y. Matsumoto, A. Shundo, M. Ohno, N. Tsuruzoe, M. Goto and K. Tanaka, *Langmuir*, 2018, **34**, 7503−7508.

15 (a) F. K. Oppong, P. Coussot and J. R. de Bruyn, *Phys. Rev. E: Stat., Nonlinear, Soft Matter Phys*., 2008, **78**, 021405; (b) T. Moschakis, A. Lazaridou and C. G. Biliaderis, *J. Colloid Interface Sci*., 2012, **375**, 50−59; (c) A. Shundo, K. Hori, D. P. Penaloza and K. Tanaka, *Rev. Sci. Instrum*., 2013, **84**, 014103-1−5.

16 (a) E. R. Weeks and D. A. Weitz, *Chem. Phys*., 2002, **284**, 361−367; (b) M. Aoki, A. Shundo, R. Kuwahara, S. Yamamoto and K. Tanaka, *Macromolecules*, 2019, **52**, 2075−2082.

17 R. Sbarbati, *Biosci. Rep*., 1985, **5**, 469−472.

18 (a) S. Shimomura, H. Matsuno and K. Tanaka, *Langmuir*, 2013, **29**, 11087−11092; (b) S. Shimomura, H. Matsuno, K. Sanada and K. Tanaka, *J. Mater. Chem. B*, 2017, **5**, 714−719; (c) S. Shimomura, H. Matsuno, Y. Kinoshita, S. Fujimura and K. Tanaka, *Polym. J*., 2018, **50**, 737–743.

19 N. G. Papadopoulos, G. V. Dedoussis, G. Spanakos, A. D.

Gritzapis, C. N. Baxevanis and M. Papamichail, *J. Immunol. Methods*, 1994, **177**, 101–111.

20 (a) G. Annadurai, R. Juang and D. Lee, *J. Hazard. Mater*., 2002, **92**, 263−274; (b) R. Batmaz, N. Mohammed, M. Zaman, G. Minhas, R. M. Berry and K. C. Tam, *Cellulose*, 2014, **21**, 1655−1665.

21 (a) N. R. Lang, S. Münster, C. Metzner, P. Krauss, S. Schürmann, J. Lange, K. E. Aifantis, O. Friedrich and B. Fabry, *Biophys. J*., 2013, **105**, 1967−1975; (b) H. C. G. de Cagny, B. E. Vos, M. Vahabi, N. A. Kurniawan, M. Doi, G. H. Koenderink, F. C. MacKintosh and D. Bonn, *Phys. Rev. Lett*. 2016, **117**, 217802.

22 Y. Matsumoto, A. Shundo, M. Ohno, N. Tsuruzoe, M. Goto and K. Tanaka, *Soft Matter*, 2017, **13**, 7433−7440.

Table of Contents

Nanocellulose-containing medium was spatially heterogeneous at a few tens of micrometres and its length scale affected the cell floating.